

PERFORMANCE OF PLAIN AND GALVANIZED REINFORCING STEEL DURING THE INITIATION STAGE OF CORROSION IN CONCRETE WITH POZZOLANIC ADDITIONS

Eric I. Moreno\* and Alberto A. Sagüés  
Department of Civil and Environmental Engineering  
University of South Florida  
Tampa Florida 33620  
\*Permanent Affiliation: CINVESTAV-Mérida, México

Rodney G. Powers  
Materials Office  
Florida Department of Transportation  
Gainesville, Florida 32609

ABSTRACT

The pH of the concrete pore solution is expected to be somewhat lower in concretes using pozzolanic additions than in concrete using unblended cements. Variations in pH pore solution may hold the key to explaining conflicting reports on the performance of galvanized rebar. To examine that factor, plain and galvanized rebars have been tested for over two years in concrete specimens made with cement type II, with various contents of fly ash and silica fume. Electrochemical impedance measurements and sensitive polarization techniques have been used to measure the rate of metal dissolution in the absence of chloride contamination at two different levels of concrete moisture. The plain steel specimens have shown little tendency for passivation in two of the cement compositions with the highest levels of pozzolanic addition. The galvanized steel passivated in all cases and showed apparent corrosion current densities of less than  $0.3 \mu\text{A}$  near the end of the test. Implications of the length of the corrosion initiation period and on current materials selection criteria are presented.

Keywords: concrete, corrosion, fly ash, galvanized steel, polarization resistance, reinforcing steel, silica fume.

INTRODUCTION

Long term durability goals (75 years and more) have recently become common in construction of reinforced concrete highway structures. This poses new challenges in controlling reinforcement corrosion, which remains one of the most important limiting factors of the service life of concrete.

Copyright

Long-term corrosion control approaches are relying increasingly on extending the length of the initiation period of corrosion (the length of time in which the reinforcement surface is still in the passive condition) since the propagation stage (from the start of active corrosion until damage is externally observed) tends to last relatively few years.<sup>1</sup>

Galvanized reinforcing steel bars are being newly considered for long-term durability service in chloride-induced corrosion service, specially since adverse experience with epoxy coated rebar in marine substructures<sup>2</sup> has created interest in examining alternative corrosion control methods. There are indications that the chloride concentration threshold for corrosion initiation of galvanized steel is greater than that for plain steel, with consequent extension in the length of the initiation period. However, exceptional stability of the galvanized layer inside concrete is required if the coating is expected to be effective after an initiation period that may well need to exceed 50 years. The chloride concentrations are small during the initiation period, but the galvanized layer is continuously exposed to an alkaline environment. Zn and Zn alloys exhibit amphoteric behavior, corroding actively in both acidic and likewise in highly alkaline media. In the absence of carbonation, the pH of concrete pore solutions is usually sufficiently high to prevent acidic corrosion, but excessive corrosion due to a too high pH is a distinct danger. In an extensive series of experiments Andrade and coworkers have shown that a continuous passivating layer of calcium hydroxyzincate forms on the surface of galvanized steel when the pH is  $13.3 \pm 0.1$  or below.<sup>3,4</sup> Modern concrete formulations for high durability in seawater service include commonly AASHTO Type II cement (for sulfate resistance), a low water to cement ratio, and a high cement factor with pozzolanic replacement. The latter consist of fly ash (for reduced permeability and to reduce temperature rise in mass concrete applications) and, increasingly, microsilica for early strength and reduced permeability. The pozzolanic additions consume  $\text{Ca}(\text{OH})_2$  and the reaction products may entrap alkali ions that would otherwise be present in the pore water.<sup>5,6</sup> As a result, the pH of the pore water in concretes with silica fume and fly ash additions can be significantly lower than in comparable unblended concretes.<sup>7,8</sup> Thus, there is a possibility that pozzolanic additions actually improve the performance of galvanized steel, at least by extending the initiation stage of corrosion.

The typical thickness of a galvanizing coating is in the order of 100  $\mu\text{m}$ . Therefore, corrosion average rates during a nominal 50-year initiation period should be well below 2  $\mu\text{m}/\text{y}$  to ensure that any coating at all remains in place when the chloride ion concentration begins to approach the threshold value. Requirements may be even more demanding since there is evidence that hot-dip galvanizing coatings provide the best corrosion protection when the outer coating layer (" $\eta$ ", nearly pure Zn) is still in place.<sup>3,4,9</sup> After wastage during the initial concrete curing period, the thickness of the  $\eta$  layer may be only 1/5 to 1/10 of the total galvanizing coating thickness. Thus, corrosion rates during the initiation period may need to be as small as a fraction of 1  $\mu\text{m}/\text{y}$  for successful coating performance. The purpose of this investigation was to obtain an indication of whether galvanized reinforcement could meet these low limits during the initiation stage in concretes formulated for high durability service. The behavior of plain steel with surface condition representative of construction site conditions was examined for comparison.

## PROCEDURE

### Specimens and materials

The concrete specimens were rectangular prisms (75 mm deep, 150 mm wide, and 300 mm high), with two parallel rebars of the same type, protruding 50 mm out of the top end.

The cementitious material used involves were type II, fly ash class "F", and silica fume. All materials satisfied AASHTO and/or ASTM specification for Florida Department of Transportation (FDOT) construction. The mix design used are shown in Table I. Mix designs B, C, D, and E have a total cementitious content representative of current FDOT concretes for marine substructure applications.

Eight concrete specimens (four with galvanized bars, and four with black bars) were cast for this experiment per mix design and cured for 28 days in a moist chamber. After curing, half of the specimens were allowed to dry in the lab environment (about 60% RH, 22°C). The remaining specimens were kept nearly water-saturated by wrapping them in plastic bags and frequently remoistening with distilled water spray.

Two types of rebar were used, galvanized and plain steel, both size No.4 (nominal 12.5 mm diameter). The rebar specimens were 300 mm long with a 212 mm unmasked length (surface area of 86 cm<sup>2</sup>) directly in contact with concrete. The rebars were cast 75 mm apart in the concrete specimens. An activated titanium rod reference electrode,<sup>10</sup> 3 mm diameter, 50 mm long, was cast centered in each concrete specimen.

The galvanized rebars were hot-dip galvanized, with an average coating thickness of 90µm, as determined by metallographic examination. The thickness of the η layer was typically 25µm. Preparation of the bars followed generally ASTM Specification A 767, but no chromate treatment was used after galvanizing. To simulate construction site conditions, the plain steel bars were cast in the as-received condition, in which an orange rust layer was present. Metallographic examination showed some mill scale still present beneath the rust.

#### pH measurements

The pH of the pore water in the concrete specimens was estimated by an in-situ leaching procedure, described in detail elsewhere.<sup>11</sup> A hole, 6.4 mm in diameter and 25 mm in depth was drilled into a cubic blank sample of each concrete mix, preconditioned by keeping it in a 100% RH chamber for ~ 1 month. Distilled water (0.4 cc) was introduced in the bottom of the orifice, and the pH of the water was periodically determined in-situ with a micro pH electrode calibrated in high pH buffer solutions. The pH measurements were continued over a period of several weeks until a stable terminal pH value was observed. This value was reported as the result of the test (average of two orifices).

#### Half cell potentials

Half cell potentials were taken regularly for each rebar against the internal reference electrode. This internal electrode was periodically calibrated against an external copper-copper sulfate electrode (CSE) placed momentarily against the external concrete surface.

#### Electrical resistance measurements

Concrete electrical resistance (R) was measured in each specimen between the two rebars. The alternating current measurement was performed using a Model 400 Nilsson soil resistivity meter. Later, R was converted to a resistivity value through a geometrical cell constant (Cc) in the following manner:

$$\rho \sim R \cdot Cc$$

The cell constant was determined to be Cc = 11 cm by calibration with rebars in a plastic cell of similar dimensions as the concrete specimens, filled with a liquid of known resistivity.

## Polarization resistance

Polarization resistance of the rebar specimens was determined by both electrochemical impedance spectroscopy (EIS), and a galvanostatic step technique.

EIS tests were conducted at an amplitude typically less than 10 mV, in the frequency interval 0.001 - 200 Hz using custom-made EIS instrumentation.

Galvanostatic step tests were performed simultaneously on groups of up to 16 specimens at the same time. The computer-controlled test technique is described in detail elsewhere.<sup>12</sup> The galvanostatic current was selected to produce a potential deviation characteristically < 20 mV. All conversions to nominal corrosion current densities and corrosion rates were made after compensation for IR drop effects.

## RESULTS

Figures 1 and 2 show the evolution of concrete resistance (average of all specimens of each concrete type and for each environmental condition) as a function of exposure time. The specimens at room humidity showed increasing resistance with time, as expected from continuing drying. The moderate long-term trend of increasing resistance of the wet specimens reflects the effect of increased curing. In both environments the highest resistivity was observed for the specimens containing the highest pozzolanic additions, specially types D and E (containing microsilica). The long term curing of the fly-ash specimens is also evident in the increased resistivity trends for the wet environment. The resistivities values ( $\rho = R \cdot 11 \text{ cm}$ ) in the wet environment are consistent with those reported in the literature for similar concretes.<sup>13</sup>

Figures 3 and 4 show the potentials (averages of quadruplicate bars) as a function of exposure time for the plain steel and galvanized specimens in the room humidity environment. Each material achieved a final potential that was approximately independent of the type of concrete. The potentials reached by each material are comparable to those reported for their respective passive conditions in dry concrete.<sup>14</sup> The early potential history of the plain steel in concrete mixes D and E (both with silica fume) was indicative of slow passivation, specially for mix D.

Figures 5 and 6 show the potential trends in the wet concretes. The galvanized specimens tended to reach final potentials (-400 to -600 mV CSE) similar to those reported elsewhere for the passive condition in wet concrete.<sup>14</sup> However, by day 750 two of the four bars in concrete mix D had reached potentials between -900 and -1000 mV CSE, resulting in a somewhat low average potential of -680 mV CSE. The plain steel specimens in concrete mixes A-C and F reached potentials (~ -100 mV CSE) associated with passive behavior<sup>15</sup> early in the exposure. In contrast, the potentials in silica-fume mixes D and E were highly negative (typ. -700 mV CSE) over the entire exposure period.

Figures 7 and 8 show the nominal corrosion rates (see discussion below), averages of quadruplicate bars for each material in the room humidity concrete tests. The galvanized rebar showed low and continually decreasing rates over the entire test interval, consistent with the potential trends shown in Figure 4. By the end of the test interval, the rates in all concrete mixes were approaching the detection limit ( $8.6 \times 10^{-3} \mu\text{m/y}$ ). The nominal corrosion rates by the end of the test interval for the plain steel in all corrosion mixes were also very low and approaching the detection limit ( $7.1 \times 10^{-3} \mu\text{m/y}$ ), in agreement with the final potential values in Figure 3. The nominal rates for mixes D and E were much higher for those periods in which potentials outside the passive regime were recorded.

Figures 9 and 10 show the nominal corrosion rates for the wet concrete tests. The galvanized specimens showed low and continually decreasing rates, generally consistent with those reported elsewhere for passive galvanized steel<sup>16</sup> in wet concrete. The specimens with concrete mix D (8% silica fume, 20% fly ash) showed throughout the test period apparent average rates ~3 times greater than those in the other concrete mixes. The plain steel specimens in mixes A-C and F showed similar, very low nominal rates over the test period, consistent with those expected from well-passivated plain steel in wet concrete.<sup>17</sup> In contrast, the plain steel in silica-fume concrete mixes D and E showed much higher nominal rates throughout the entire test interval, coincident with the observation of very negative potentials shown in Figure 5.

Table 2 shows the results of estimated pH measurements. The concrete mixes D and E showed the lowest pH values, as observed also by other investigators.<sup>7,8</sup>

## DISCUSSION

### Galvanized Steel

The accuracy of the nominal corrosion rate calculated from polarization resistance measurements is contingent upon the accuracy of the  $R_p$  measurements themselves and upon the reliability of the conversion from  $R_p$  to corrosion rate. The  $R_p$  calculations from experimental data are based on a simplified model of the interface that agrees generally with the result of more detailed electrochemical impedance tests.<sup>12</sup> Because of the large apparent interfacial capacitances of these systems, values of  $R_p$  can only be interpreted by extrapolation and thus should be considered as apparent values. The conversion from apparent polarization resistance to nominal corrosion current density was made in the passive regime by means of a Stern-Geary constant  $B=52$  mV, from which metal dissolution rates were obtained assuming double ionization of Zn. The 52 mV constant was determined empirically by Andrade et al from gravimetric measurements of passive galvanized steel using polarization resistances obtained by comparable methods.<sup>18</sup> Those investigators reported accurate corrosion rate determinations within a factor of 2. It is therefore expected that the present nominal corrosion rates of passive galvanized steel have a comparable level of error.

The above evaluation of corrosion rate does not invoke any specific mechanism for dissolution of zinc in the passive state. However, some theoretical justification for the conversion approach used may be derived by assuming that metal loss occurs by dissolution of the passive layer at the layer-pore water interface, and growth of the layer by zinc ions resulting from oxidation of the bulk metal at the layer-metal interface. If the rate of passive metal dissolution follows the potential-independent trend of an ideal passive polarization curve,<sup>19,20</sup> the electrochemical admittance of the overall anodic reaction is zero, and the overall admittance at the polarization resistance limit is that of the cathodic reaction. Assuming it to be simple oxygen reduction, not limited by diffusion since the reaction rate is low, the polarization resistance would be given by  $R_p = \beta/2.3 i_{\text{corr}}$ , where  $\beta$  is the Tafel slope of the cathodic reaction. Therefore the Stern-Geary constant is  $B = \beta/2.3$ , which for  $B=52$  mV yields  $\beta = 0.12$  V, a value which is consistent with the independently observed typical kinetic parameters for oxygen reduction in concrete.<sup>21</sup>

The potential and nominal corrosion rate results suggest that the galvanized steel has developed stable passivity after two years in all concrete mixes in the room humidity concrete, and in mixes A-C and E-F in wet concrete. The potential of two of the galvanized specimens in wet mix D concrete fell outside the range normally associated with passivity, but the nominal corrosion rates for those specimens were found to be similar to those of the other specimens in the same group which retained potentials in

the normal passive regime. The average nominal corrosion rates for all the galvanized specimens show a tendency to decrease with time in both environments.

Galvanized reinforcement is being evaluated in this investigation primarily for its expected resistance to higher levels (compared with plain steel) of chloride ion contamination before initiation of the active corrosion. An increased contamination threshold means that longer time would be required for diffusion or other transport processes to build up the necessary critical chloride concentration at the rebar level, thus increasing durability with respect to plain rebar construction. Therefore, the ability of the galvanizing coating to be present to the end of a long initiation period is essential. Keeping the limitations of the test techniques in mind, the results in Figure 10 show nominal rates of metal wastage after two years in the galvanized specimens in mix D wet concrete of less than  $0.3 \mu\text{m/y}$ . The nominal corrosion rates after two years were less than about  $0.12 \mu\text{m/y}$  for mixes A, F, C, and E. Considering the observed trend for increasingly smaller nominal corrosion rates with time, the results suggest that a usable fraction of even the small  $\eta$  layer thickness could remain in place after 50 years of initiation service. Penetration through the remaining galvanized layers<sup>22,23</sup> would be expected to involve longer time periods. The performance in concrete exposed to room humidity appears to be significantly better than in wet concrete, with consequent increase in the chances of survival after a long initiation period.

The results to date suggest that the pozzolanic additions tested do not create an environment aggressive to galvanized steel. From the pH estimates in Table 2, the pozzolanes may actually assist in keeping the pore solution away from the aggressive pH limit of 13.3 suggested by Andrade et al.<sup>3</sup> There is no clear indication that too much of a reduction in pH from the pozzolanic reaction may be taking place, but the behavior of galvanized steel in concrete mix D (low potentials in some specimens) must be monitored with attention in the future.

The scope of the above discussion is limited to the survival of the galvanizing coating during the initiation stage of corrosion, when chloride ion levels are small for a large portion of the time and assuming that the concrete does not contain cast-in chloride contamination. The effect of rapidly increasing levels of contamination near the end of the initiation stage has not been yet considered as it is expected to involve a relatively small fraction of the total initiation time. Cases of initial contamination and the effect of very small chloride levels during buildup should be examined in the future. The performance of galvanized steel in the propagation stage of corrosion is being investigated in related experiments to be reported elsewhere.

#### Plain steel

The behavior of the plain steel bars was as expected in the case of mixes A,F and B,C, yielding very low nominal corrosion rates for both wet and room humidity concretes. The estimation of nominal corrosion rates is based on empirical "B" constants (52 mV for passive steel and 26 mV for active steel) reported in the literature,<sup>24</sup> and it is expected that reasonable estimates were obtained for specimens in the passive condition. In silica-fume mixtures D and E, in wet concrete, conditions normally associated with passivity were never reached. In dry concrete those conditions developed only after relatively long periods. These anomalous behaviors are puzzling.

The nominal corrosion rates reported for the anomalous behavior in mixes D and E cannot be substantiated at this time and must be considered only as apparent magnitudes. Several causes of uncertainty exist. EIS tests of specimens in the anomalous conditions suggest the presence of a very low apparent polarization resistance, but because of the comparatively high electrolyte resistance not enough resolution could be obtained to provide an accurate estimate of  $R_p$  (additional testing is in progress to

determine the EIS response with greater precision). Similar inaccuracy affects the anomalous condition  $R_p$  values from the galvanostatic tests, which can only be considered as order-of-magnitude estimates. A more important uncertainty concerns the cause of the low apparent polarization resistance. It may be due to only high corrosion rate of the steel, which would not have yet experienced passivation in the lower pH environment of the mixtures with highest and most reactive pozzolanic addition. However, even the lowest pH values observed (12.6, mix E, Table 2) could be expected to cause passivity after a relatively short time. Moreover, sustained corrosion rates on the order of 25  $\mu\text{m}/\text{y}$  may cause visible cracking of the concrete cover after two years in the specimen configuration used,<sup>25</sup> but no cracking was observed.

An alternative interpretation can be proposed based on the initial, red rust condition of the plain steel specimens. If this surface layer is rich in  $\text{Fe}^{+++}$  ions, reduction to  $\text{Fe}^{++}$  may be expected as a possible cathodic reaction in concrete.<sup>26</sup> This cathodic reaction could be matched by conversion to a higher oxidation state of oxides in the mill scale, and/or the base metal, until an equilibrium is reached followed by formation of the usual passive condition. The lower pH expected (and observed) of the high pozzolanic concrete mixes would have retarded passivation in the normal manner, allowing for the development of processes such as the one proposed. The standard  $\text{Fe}^{+++}/\text{Fe}^{++}$  equilibrium in aqueous solution at pH 12-13 takes place at potentials approaching -900 mV CSE,<sup>27</sup> which would be consistent with the observed potential values. A red rust layer 50-100  $\mu\text{m}$  thick could provide ample material to support electrochemical reaction rates on the order of those observed for times comparable to the duration of the test. Strain relief (and consequent lack of cracks) is conceivable given the friable and porous nature of the rust layer and the combinations of possible volume changes involved in oxide transformations. In the wet specimens oxygen availability is limited by slow diffusion through the concrete, and the low potential regime would be expected to last longer than in the drier specimens, as observed. Because of the increasing use of silica fume for long term durability applications, resolution of the behavior of these specimens is important. Careful monitoring for longer times and demolition of selected specimens is planned to elucidate these possibilities.

## CONCLUSIONS

1. Galvanized steel in chloride-free concretes with a range of pozzolanic additions reached passive behavior in both wet and dry conditions. Apparent corrosion rates after two years of exposure were very low ( $<0.3 \mu\text{m}/\text{y}$ ), suggesting that a significant portion of the  $\eta$  layer could remain in place for a period on the order of 50 years before the arrival of a chloride contamination front.
2. The estimated pH of the pore solutions in the concretes used was below the 13.3 limit suggested for lack of stability of the galvanized layer. The estimated pH was lowest with the highest pozzolanic content, suggesting that the pozzolanic additions might assist in improving the coating stability. However, galvanized reinforcing steel in one of the high pozzolanic mixes with silica fume showed the highest passive corrosion rate and low potentials (but still passive corrosion rates) in a fraction of its samples. Longer-term monitoring is continuing.
3. Plain steel controls showed passivation and very low corrosion rates after two years in the dry environment for all concrete mixes, and in the wet conditions for mixes without silica fume. However, the plain steel bars in the wet silica fume concretes did not show potentials or apparent corrosion rates indicative of passivity even after two years. The presence of an initial red rust layer on the plain steel specimens, coupled with reduced pore water pH in these concretes was proposed as a possible cause of this behavior.

## ACKNOWLEDGMENT

This investigation was supported by the Florida Department of Transportation. The opinions, findings, and conclusions expressed here are those of the authors and not necessarily those of the Florida Department of Transportation. The authors are indebted to Dr. S. Kranc for his valuable assistance in programming the reduction of extensive polarization data sets. One of the authors (E.I.M.) acknowledges the scholarship provided by the National Council of Science and Technology (CONACYT-México).

## REFERENCES

1. R. Weyers, B. Prowell, I. Al-Qadi, M. Sprinkel, M. Vorster, "Concrete Bridge Protection, Repair, and Rehabilitation Relative to Reinforcement Corrosion," Strategic Highway Research Program, SHRP-S-360, March 30, 1993.
2. A. Sagüés, R. Powers, R. Kessler, "Corrosion Processes and Field Performance of Epoxy-Coated Reinforcing Steel in Marine Substructures," CORROSION/94, paper no. 299 (Houston, TX: NACE, 1994).
3. A. Macías, C. Andrade, *Brit. Corros. J.*, 18, 2 (1983): p. 82.
4. M. Blanco, C. Andrade, A. Macías, *Brit. Corros. J.*, 19, 1 (1984): p. 41.
5. S. Diamond, *Cem. Concr. Res.*, 11, 3 (1981): p. 383.
6. S. Diamond, *J. Am. Ceram. Soc.*, 66, 5 (1983): p. C-82.
7. K. Andersson, B. Allard, M. Bengtsson, B. Magnusson, *Cem. Concr. Res.*, 19, 3 (1989): p. 327.
8. U. Wiens, W. Breit, P. Schiessl, in *Fly Ash, Silica Fume, Slag, and Natural Pozzolans in Concrete*, ed. V.M. Malhotra, vol. 2 (Detroit, MI: ACI, 1995), p. 741.
9. C. Andrade, A. Macías, in *Surface Coatings-2*, eds. A. Wilson, J. Nicholson, H. Prosser (London, UK: Elsevier Applied Science, 1988): p. 137.
10. P. Castro, A. Sagüés, E. Moreno, L. Maldonado, J. Genésca, *Corrosion*, 52 (1996): in press.
11. A. Sagüés, E. Moreno, C. Andrade, in preparation.
12. A. Sagüés, S. Kranc, E. Moreno, *Electrochim. Acta* (1995): in press.
13. N. Berke, M. Hicks, in *Corrosion Forms and Control for Infrastructure*, ASTM STP-1137, ed. V. Chaker (Philadelphia, PA: ASTM, 1992): p. 207.
14. J. González, C. Andrade, *Brit. Corros. J.*, 17, 1 (1982): p. 21.
15. ACI Publication 222R-89, "Corrosion of Metals in Concrete" (Detroit, MI: ACI, 1989).
16. J. González, A. Vázquez, G. Jauregui, C. Andrade, *Matér. Constr. (Paris)*, 17, 102 (1984): p. 409.



17. W. López, J. González, *Cem. Concr. Res.*, 23, 2 (1993): p. 368.
18. A. Macias, C. Andrade, *Corros. Sci.*, 30, 4/5 (1990): p. 393.
19. F. Mansfeld, in *Advances in Corrosion Science and Technology*, eds. M. Fontana, R. Staehle (New York, NY: Plenum Press, 1976).
20. S. Pyun, J. Bae, S. Park, J. Kim, H. Lee, *Corros. Sci.*, 36, 5 (1994): p. 827.
21. A. Sagüés, S. Kranc, A. Al-Mansur, S. Hierholzer, "Factors Controlling Corrosion of Steel-Reinforced Concrete Substructure in Seawater", *Nat. Tech. Inf. Service*, FL/DOT/RC/0537-3523, June 1994.
22. S. Yeomans, *Corrosion*, 50, 1 (1994): p. 72.
23. S. Yeomans, in *Corrosion and Corrosion Protection of Steel in Concrete*, ed. R.N. Swamy, vol. 2 (Sheffield, UK: Sheffield Academic Press, 1994): p. 1299.
24. C. Alonso, C. Andrade, J. González, *Cem. Concr. Res.* 18, 5 (1988): p. 687.
25. C. Andrade, M. Alonso, in *Application of Accelerated Corrosion Tests to Service Life Prediction of Materials*, ASTM STP-1194, eds. G. Cragolino, N. Sridhar (Philadelphia, PA: ASTM, 1994): p. 282.
26. J. Avila-Mendoza, J. Flores, U. Castillo, *Corrosion*, 50, 11 (1994): p. 879.
27. M. Pourbaix, *Atlas of Electrochemical Equilibria in Aqueous Solutions* (Houston, TX: NACE, 1974).

**TABLE 1**  
**Concrete Mix and Properties**

Mixes	Cementitious Material	Cementitious content (Kg/m <sup>3</sup> )	Water to Cementitious Ratio	Measured Strength 28 day (MPa)
A	100%PC	333	0.55	37
F	100%PC	360	0.41	34 *
B	80%PC + 20%FA	444	0.41	46
C	70%PC + 30%FA	444	0.43	42
D	72%PC + 20%FA + 8%MS	444	0.39	58
E	62%PC + 30%FA + 8%MS	444	0.39	56

PC = Portland Cement Type II; FA = Fly Ash Class "F"; MS = Micro Silica.

\* Design, measured not available.

**TABLE 2**  
**Concrete pH Pore Solution**

Mixes	Estimated pH
A	13.02
F	13.04
B	13.00
C	13.02
D	12.92
E	12.66

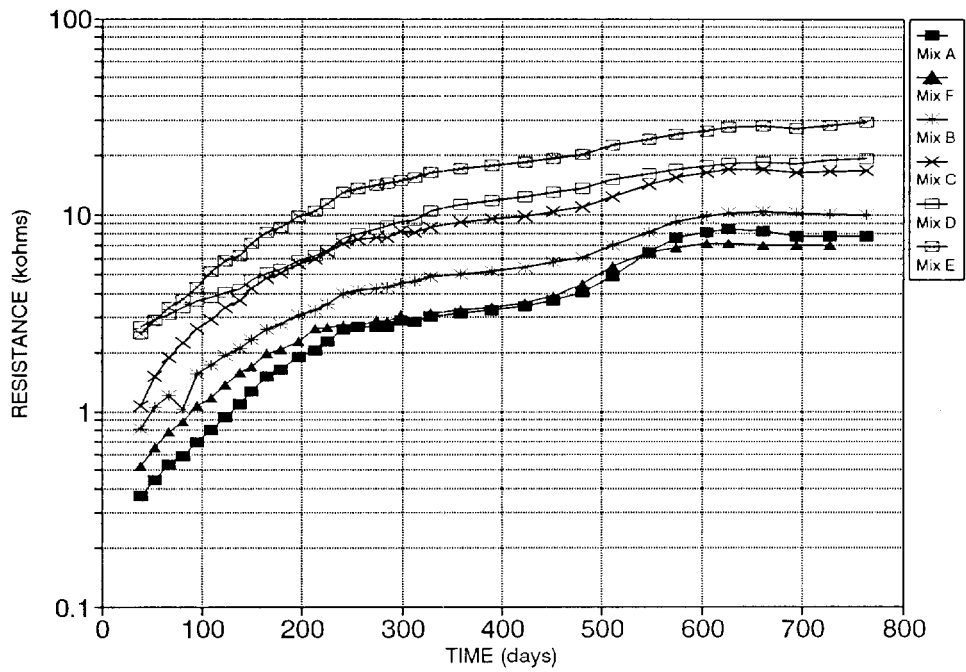


Figure 1. Evolution of concrete resistance in the laboratory air environment, as a function of exposure time (Resistivity  $\rho \sim R \times 11 \text{ cm}$ ).

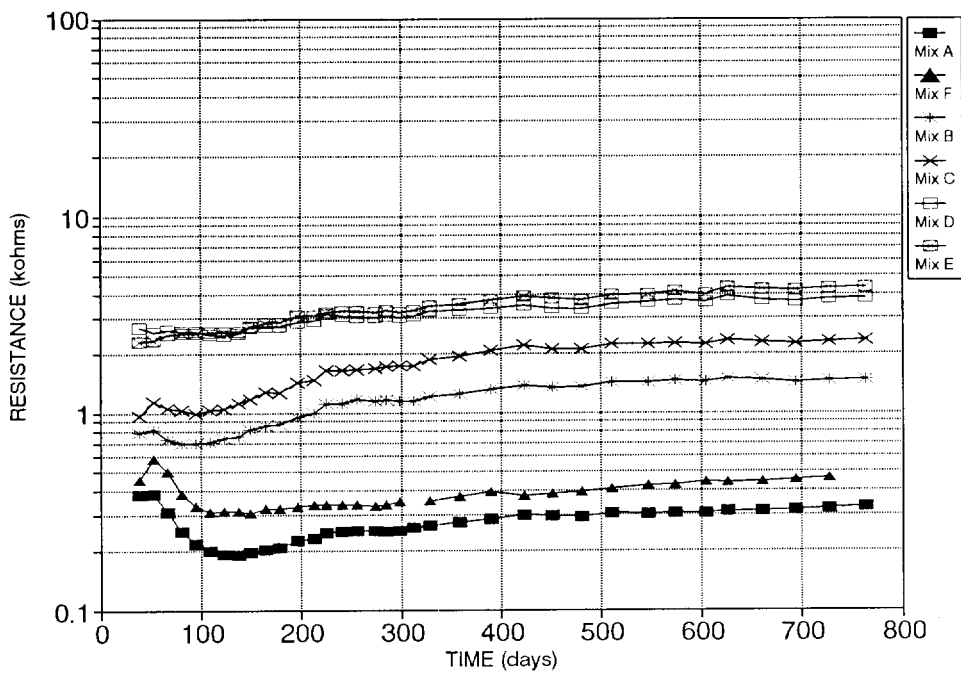


Figure 2. Evolution of concrete resistance in the wet specimens, as a function of exposure time (Resistivity  $\rho \sim R \times 11 \text{ cm}$ ).

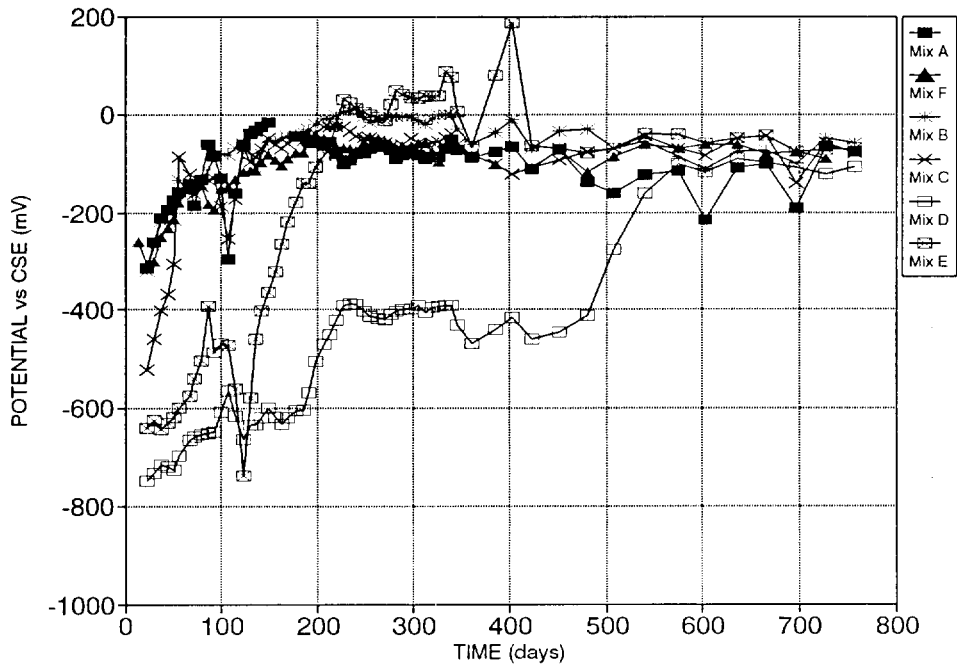


Figure 3. Potentials as a function of exposure time for the plain steel in the laboratory air concrete specimens.

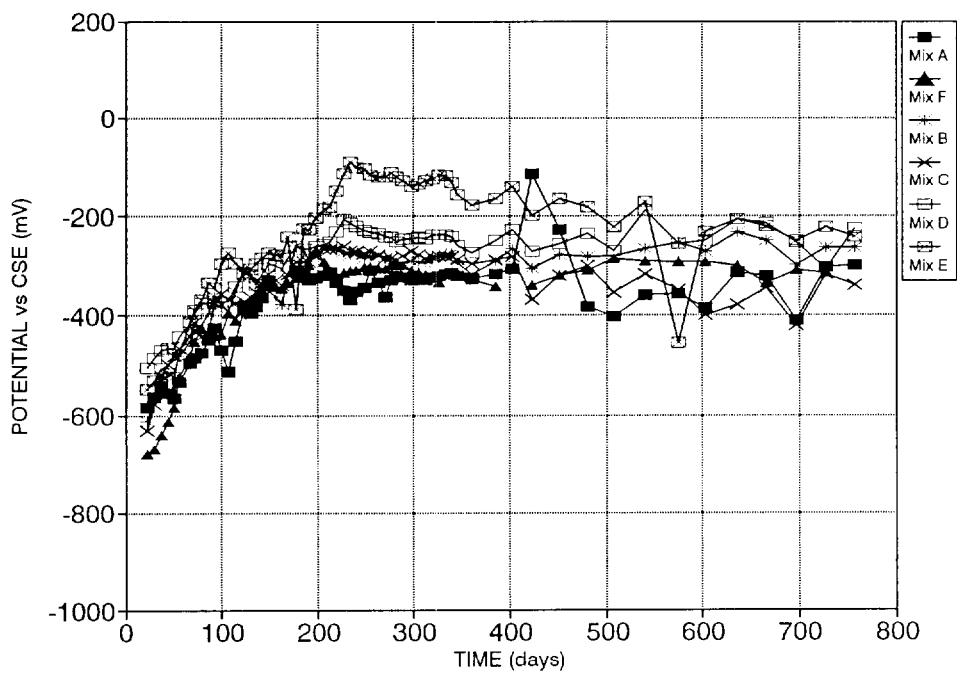


Figure 4. Potentials as a function of exposure time for the galvanized steel in the laboratory air concrete specimens.



Figure 5. Potentials as a function of exposure time for the plain steel in the wet concrete specimens.

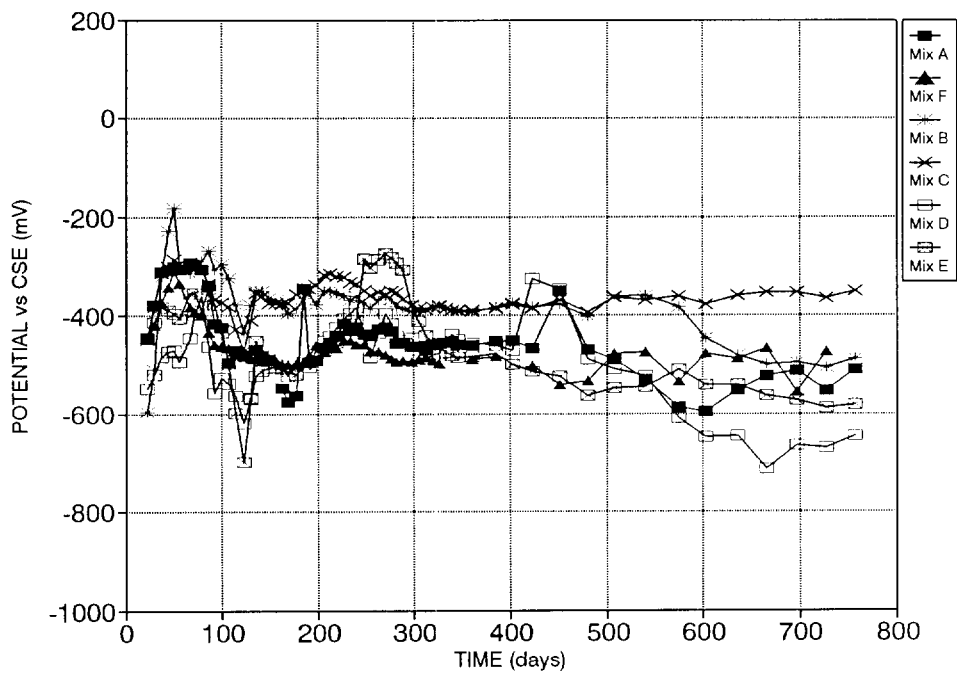


Figure 6. Potentials as a function of exposure time for the galvanized steel in the wet concrete specimens.

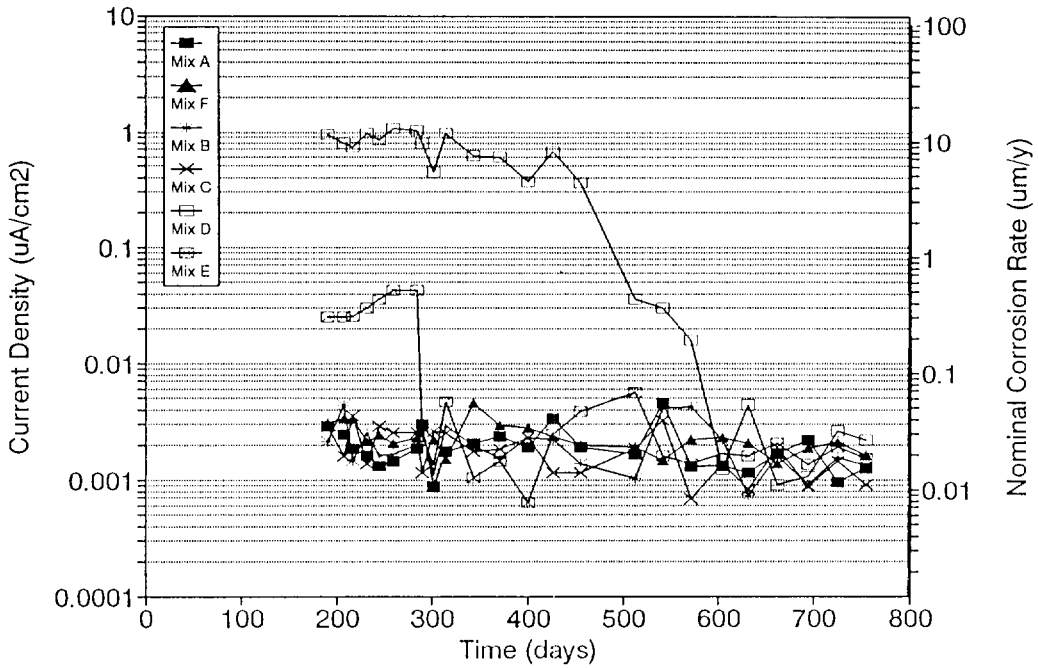


Figure 7. Evolution of the current densities and nominal corrosion rates as a function of exposure time for the plain steel in the laboratory air concrete specimens. See text for interpretation of the high apparent rates for mixes D and E.

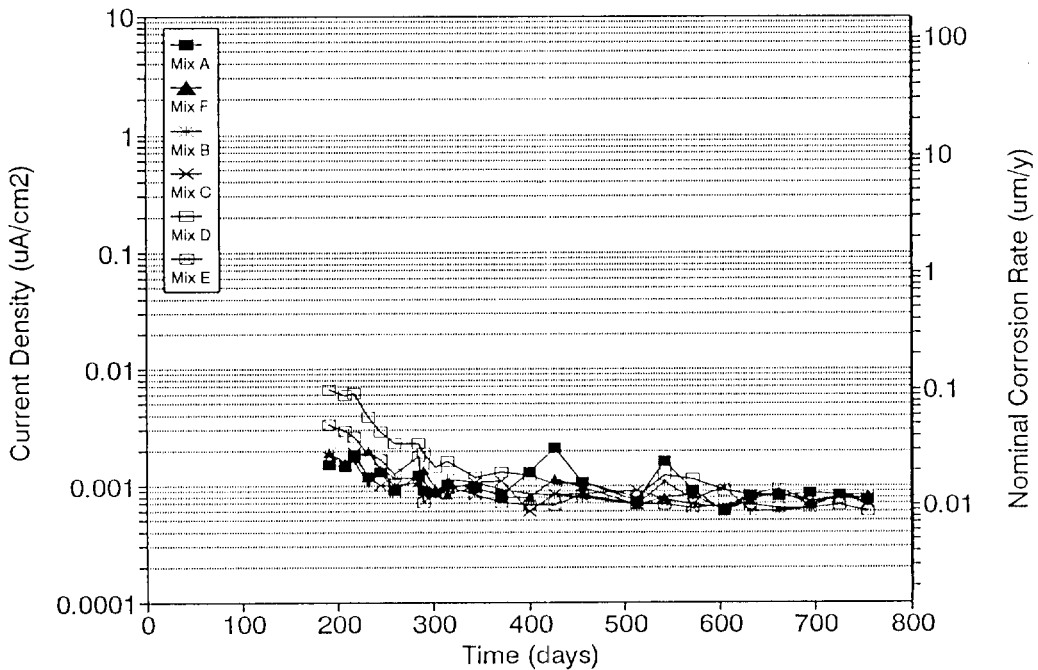


Figure 8. Evolution of the current densities and nominal corrosion rates as a function of exposure time for the galvanized steel in the laboratory air concrete specimens.

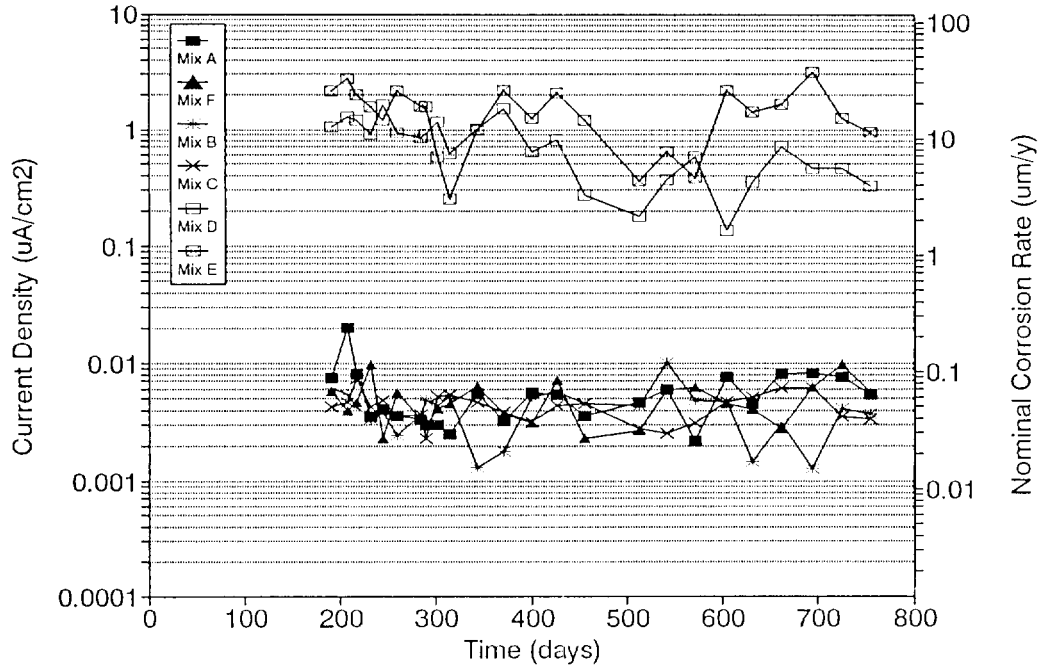


Figure 9. Evolution of the current densities and nominal corrosion rates as a function of exposure time for the plain steel in the wet concrete specimens.

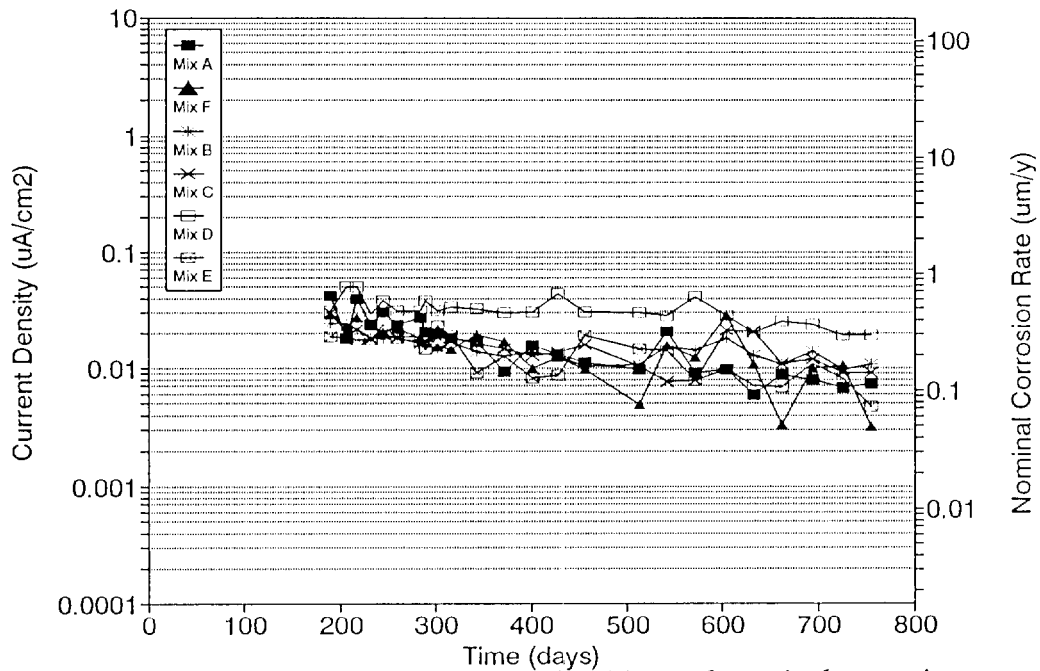


Figure 10. Evolution of the current densities and nominal corrosion rates as a function of exposure time for the galvanized steel in the wet concrete specimens.